

Generation of quasi-chirp-free isolated attosecond pulses from atoms under the action of orthogonal two-color combined pulse of fundamental frequency and higher intensity second harmonic fields

Rui-Xian Yu(蔚瑞贤), Yue Qiao(乔月), Ping Li(李萍), Jun Wang(王俊), Ji-Gen Chen(陈基根), Wei Feng(冯伟), Fu-Ming Guo(郭福明), and Yu-Jun Yang(杨玉军)

Citation: Chin. Phys. B, 2023, 32 (**6**): 063302. DOI: 10.1088/1674-1056/acc80a
Journal homepage: http://cpb.iphy.ac.cn; http://iopscience.iop.org/cpb

What follows is a list of articles you may be interested in

Amplitude and rotation of the ellipticity of harmonicsfrom a linearly polarized laser field

Ping Li(李萍), Na Gao(高娜), Rui-Xian Yu(蔚瑞贤), Jun Wang(王俊), Su-Yu Li(李苏宇), Fu-Ming Guo(郭福明), and Yu-Jun Yang(杨玉军)

Chin. Phys. B, 2022, 31 (**10**): 103303. DOI: 10.1088/1674-1056/ac8ce8

Enhancement of isolated attosecond pulse generation by using long gas medium

Yueying Liang(梁玥瑛), Xinkui He(贺新奎), Kun Zhao(赵昆), Hao Teng(滕浩), and Zhiyi Wei(魏志义)

Chin. Phys. B, 2022, 31 (**4**): 043302. DOI: 10.1088/1674-1056/ac29a8

Decoding the electron dynamics in high-order harmonic generation from asymmetric molecular ions in elliptically polarized laser fields

Cai-Ping Zhang(张彩萍) and Xiang-Yang Miao(苗向阳)

Chin. Phys. B, 2022, 31 (**4**): 043301. DOI: 10.1088/1674-1056/ac29b0

Review on non-dipole effects in ionization and harmonic generation of atoms and molecules

Mu-Xue Wang(王慕雪), Si-Ge Chen(陈思格), Hao Liang(梁昊), Liang-You Peng(彭良友)

Chin. Phys. B, 2020, 29 (**1**): 013302. DOI: 10.1088/1674-1056/ab5c10

Influence of the initial electronic state on minima of high-order harmonic spectrum radiated from hydrogen molecular ion

Hui-Fang Cui(崔会芳), Xiang-Yang Miao(苗向阳)

Chin. Phys. B, 2017, 26 (**10**): 103302. DOI: 10.1088/1674-1056/26/10/103302

Generation of quasi-chirp-free isolated attosecond pulses from atoms under the action of orthogonal two-color combined pulse of fundamental frequency and higher intensity second harmonic fields

Rui-Xian Yu(蔚瑞贤)[1,2], Yue Qiao(乔月)[1,2], Ping Li(李萍)[1,2], Jun Wang(王俊)[1,2], Ji-Gen Chen(陈基根)[3], Wei Feng(冯伟)[1,2,†], Fu-Ming Guo(郭福明)[1,2,‡], and Yu-Jun Yang(杨玉军)[1,2,§]

[1] *Institute of Atomic and Molecular Physics, Jilin University, Changchun* 130012, *China*
[2] *Jilin Provincial Key Laboratory of Applied Atomic and Molecular Spectroscopy (Jilin University), Changchun* 130012, *China*
[3] *Zhejiang Provincial Key Laboratory for Cutting Tools, Taizhou University, Jiaojiang* 31800, *China*

(Received 20 February 2023; revised manuscript received 17 March 2023; accepted manuscript online 28 March 2023)

The intrinsic chirp of high-order harmonic generation is an important factor limiting the production of ultrashort attosecond pulses. Based on numerically solving the time-dependent Schrödinger equation, the generation process of high-order harmonic from the He atom under the action of orthogonal two-color combined pulse of fundamental frequency and higher intensity second harmonic fields is studied. In this paper, we propose to achieve quasi-chirp-free isolated attosecond pulses by superimposing a higher second-harmonic field on the orthogonal direction of the fundamental frequency field. It is found that the high-energy part of its harmonic emission exhibits small chirp characteristics, which can be used to synthesize isolated attosecond pulses. Through the analysis of the wave packets evolution and the classical motion trajectories of the electron, it is demonstrated that the quasi-chirp-free harmonic can be attributed to the simultaneous return of electrons ionized at different times to the parent particle. The influence of the relative phase of the two pulses on the harmonics is further analyzed, and it is observed that this phenomenon is sensitive to the relative phase, but it can still generate isolated attosecond pulses within a certain phase.

Keywords: high-order harmonic, orthogonal two-color fields, relative phase, quasi-chirp-free isolated attosecond pulses

PACS: 33.20.Xx, 42.65.Ky **DOI:** 10.1088/1674-1056/acc80a

1. Introduction

High-order harmonic generation (HHG) can be observed when ultrashort intense laser pulses interact with atoms, molecules, and solids.[1–16] The central wavelength of HHG can reach extreme ultraviolet and even x-ray band, it can be used to study ultrafast molecular, plasma, and material dynamics,[17,18] characterize nanoscale heat flow,[19] track the dynamics of specific elements in magnetic materials,[20] and nanometer resolution coherent diffraction imaging,[21] *etc*. Due to the large bandwidth of its emission spectrum, HHG has become one of the main means to obtain attosecond pulses,[22–24] and it has a wide range of applications for ultrafast holography and tracking ultrafast dynamics of an electron in atoms.[24,25]

HHG is highly nonlinear, and the process of the HHG can be well explained by a semi-classical three-step model.[26,27] Under the action of a strong laser pulse, the potential barrier is strongly distorted, and the bound electron has a certain probability to tunnel out from the potential barrier and become ionized; then the ionized electron is accelerated in the laser field to gain energy; and finally some electrons have the opportunity to move again to the nuclear region and recollide with their parent ion, and then emit high-energy photons. Due to the electron can ionize at different times, the recolliding time of the ionized electron under the action of driving light is different. Therefore, the harmonic light emission carries an inherent chirp.[25,28]

The generation of isolated attosecond pulses that reach the Fourier transform limit is restricted by the presence of harmonic chirps. At present, the maximum harmonic energy that can be obtained in the laboratory has reached 1.6 keV,[29] while the shortest isolated attosecond pulses that can be characterized is 43 attoseconds,[30] which is much larger than the Fourier-transform-limited pulses width corresponding to this energy width spectrum. In order to obtain the shorter isolated attosecond pulses, the chirp of the harmonic needs to be compensated. Usually, the harmonic chirp compensation scheme is implemented after the harmonic generation. Experimentally, compensating the positive chirp of harmonic is achieved mainly by using two techniques, the chirp multi-

†Corresponding author. E-mail: fengw@jlu.edu.cn
‡Corresponding author. E-mail: guofm@jlu.edu.cn
§Corresponding author. E-mail: yangyj@jlu.edu.cn

© 2023 Chinese Physical Society and IOP Publishing Ltd

layer x-ray mirror[31] and the negative group delay dispersion (GDD),[32] the harmonic pulses are compressed by using the dispersive material elements of the metal thin film[33] or gas medium.[34,35] The first technique uses a chirped multilayer mirror which has a small reflection bandwidth and is difficult to fabricate; the second technique depends on the dispersive properties of the transmission material, the suitable spectral region for chirp compensation is limited, and it is difficult for GDD to realize negative chirp compensation in XUV region.

From the above discussion, it can be seen that the compensation after harmonic generation requires a deep understanding of the space–time characteristics of harmonic to achieve better compensation, so there are certain limitations. If the electric field that generates harmonics is regulated so that the harmonics have no chirp or very small chirp, then an isolated attosecond pulse with a shorter duration can be obtained without further compensation. Zou *et al*. used the combined pulse of linear chirped fundamental frequency and its sub-harmonic laser pulses to drive an atom and saw that the inherent chirp of harmonic emission was significantly reduced, and the time synchronization of the harmonic emission of different photon energies was realized.[36] Kohler *et al*. proposed for arbitrarily engineering the high-order harmonic generation phase achieved by adding the first 8 Fourier components to a sinusoidal field, and employ x-rays to ionize the electron with non-zero velocity and combine it with femtosecond pulse shaping to control the spectral phase of the harmonic spectrum, the bandwidth-limited emission of 8 attoseconds is shown from Li^{2+} gas.[37] People have theoretically studied the HHG of the inhomogeneous field[38] and terahertz field,[39–42] it is also found that the reduction of the harmonic chirp by using the spatially inhomogeneous electric field and the terahertz field added with infrared laser can produce the supercontinuum harmonics spectrum with lower chirp and wider bandwidth, and isolated attosecond pulses can be synthesized using these supercontinuum harmonics. These schemes require the use of high-intensity and ultra-short THZ or the preparation of a spatially inhomogeneous field, which poses certain challenges to experiments.

In recent years, people have made a lot of achievements by using orthogonal polarization two-color fields. Not only a great improvement in harmonic efficiency was observed,[43] but also a strong attosecond pulse train was generated.[44] However, these works do not study the effect on harmonic chirp. A weak second-harmonic laser field is added to the driving laser field, Zheng *et al*. found that the chirp was compensated in the 10th harmonic range, and the pulse width of the reconstructed attosecond pulse train can be close to the Fourier-transform-limited pulse.[45] However, this scheme has not been effectively applied to the generation of chirp-free isolated attosecond pulses. The limitation of the application of this scheme can be partly attributed to the lack of in-depth understanding of the physical mechanism of reducing harmonic chirp and the lack of targeted light field regulation. How to conveniently obtain broadband high-order harmonic radiation with a small chirp or even chirp-free is still the goal pursued by people.

To solve this problem, we have conducted in-depth research and found that quasi-chirp-free isolated attosecond pulses cannot be observed by using orthogonal weak second harmonics in our simulation parameters. It is also found that under the orthogonal action of higher intensity second-harmonic and fundamental frequency fields, the quasi-chirp-free attosecond pulse can be generated. More importantly, in this paper we give the mechanism of reducing harmonic chirp by combining the motion of electron wave packet with the time–frequency behavior of harmonic emission, which lays a theoretical foundation for the experimental generation of isolated attosecond pulses without chirp, and can be targeted to design experiments. In the second part of the paper, we introduce the theoretical method used to simulate the harmonic emission, the third part gives our theoretical simulation results and related discussions and analysis, and the last part is a summary of our research work. Unless otherwise specified, the physical quantities throughout the text are in atomic units.

2. Theoretical model and method

Under the dipole approximation and the length gauge, the behavior of the He atom driven by an orthogonal two-color field satisfies the following time-dependent Schrödinger equation (TDSE):

$$\mathrm{i}\frac{\partial}{\partial t}\psi(\boldsymbol{r},t)=\left[-\frac{1}{2}\nabla^2+V(\boldsymbol{r})+\boldsymbol{E}(t)\cdot\boldsymbol{r}\right]\psi(\boldsymbol{r},t). \quad (1)$$

The soft-core Coulomb potential can be expressed as

$$V(x,y)=-\frac{Q}{\sqrt{x^2+y^2+A}}, \quad (2)$$

where $A=0.6$ is the parameter of the softcore Coulomb potential and $Q=1.5$ is the effective nuclear charge number. The electric field vector of the orthogonal two-color linearly polarized pulse is $\boldsymbol{E}(t)=E_x(t)\hat{e}_x+E_y(t)\hat{e}_y$, $E_x(t)$ and $E_y(t)$ are the x and y components of the orthogonal two-color linearly polarized pulses electric field vector, and the specific form is as follows:

$$E_x(t)=E_1 f(t)\cos(\omega t+\varphi),\quad E_y(t)=E_2 f(t)\cos(2\omega t), \quad (3)$$

where $f(t)$ is a Gaussian envelope with a full width at half maximum (FWHM) of 7 cycles, E_1 and E_2 are the peak amplitudes of fundamental frequency and double frequency laser pulses, respectively. ω is the angular frequency of the driving laser pulse. φ represents the relative phase between two directional laser fields.

The spatial wave function $\psi(\boldsymbol{r},t)$ at any instant can be obtained by solving Eq. (1) using the split operator method. By using the obtained wave function, the time-dependent dipole accelerations matrix elements in the x and y directions can be calculated

$$\begin{aligned} a_x(t) &= \frac{\mathrm{d}^2}{\mathrm{d}t^2}\langle\psi(x,y,t)\,|x|\,\psi(x,y,t)\rangle \\ &= \left\langle\psi(x,y,t)\right|-\frac{\partial V(x,y)}{\partial x}-E_x(t)\left|\psi(x,y,t)\right\rangle, \\ a_y(t) &= \frac{\mathrm{d}^2}{\mathrm{d}t^2}\langle\psi(x,y,t)\,|y|\,\psi(x,y,t)\rangle \\ &= \left\langle\psi(x,y,t)\right|-\frac{\partial V(x,y)}{\partial y}-E_y(t)\left|\psi(x,y,t)\right\rangle. \end{aligned} \tag{4}$$

The time–frequency Fourier transform is performed on the above formula to obtain the corresponding high-order harmonic spectrum

$$\begin{aligned} P_{a_x}(\omega) &= \left|\frac{1}{\omega^2(t_n-t_0)}\int_{t_0}^{t_n} a_x(t)\,\mathrm{e}^{-\mathrm{i}\omega t}\,\mathrm{d}t\right|^2, \\ P_{a_y}(\omega) &= \left|\frac{1}{\omega^2(t_n-t_0)}\int_{t_0}^{t_n} a_y(t)\,\mathrm{e}^{-\mathrm{i}\omega t}\,\mathrm{d}t\right|^2. \end{aligned} \tag{5}$$

Attosecond pulses can be obtained by superimposing harmonics within a certain order range, and the distribution in the time domain is

$$I(t) = \left|\sum_q a_q\,\mathrm{e}^{\mathrm{i}q\omega t}\right|^2, \tag{6}$$

where q is the order of harmonics, $a_q = \int a(t)\,\mathrm{e}^{-\mathrm{i}q\omega t}\,\mathrm{d}t$. By using wavelet transform, the physical mechanism of high-order harmonic emission can be analyzed from time–domain and frequency–domain information. The specific formula is

$$A_\omega(t_0,\omega) = \int_{t_\mathrm{i}}^{t_\mathrm{f}} a(t) w_{t_0,\omega}(t)\,\mathrm{d}t, \tag{7}$$

$|A(t_0,\omega_0)|^2$ represents the change information of HHG intensity with time and frequency, $w_{t_0,\omega}(t) = \sqrt{\omega}W\left[\omega(t-t_0)\right]$ is the kernel of the wavelet transform, $W(x)$ is the Morlet wavelet[46–48]

$$W(x) = \frac{1}{\sqrt{\tau}}\,\mathrm{e}^{\mathrm{i}x}\,\mathrm{e}^{-x^2/2\tau^2}. \tag{8}$$

To understand the process of HHG, we also simulate the motion of ionized electrons driven by intense laser pulses by solving the classical Newtonian equation of motion

$$\begin{aligned} \ddot{x} &= -\frac{\partial V(x,y)}{\partial x} - E_x(t), \\ \ddot{y} &= -\frac{\partial V(x,y)}{\partial y} - E_y(t). \end{aligned} \tag{9}$$

3. Results and analysis

The wavelength of the fundamental frequency laser is 800 nm, and the frequency of the orthogonal laser pulses is double the fundamental frequency, the peak amplitude of the laser intensities for the fundamental frequency E_1 and the double frequency E_2 are both 0.11 (corresponding to the intensity of $I = 3.95\times10^{14}$ W/cm^2), the change of the laser field strength vector with time is shown in the inset of Fig. 1, and the relative phase between the fundamental frequency field and the second one is 0.375 π. In the figure, the blue line represents its projection on E_x and E_y planes, the black line indicates that E_x changes with time and the green line indicates that E_y changes with time. The high-order harmonic emission spectrum of the He atom produced by this combined laser pulse is shown in Fig. 1. The black solid line is the high-order harmonic emission spectrum of the x-direction component; the red dashed line is the high-order harmonic emission spectrum of the y-direction component. It can be found from the figure that the harmonic intensity in the y direction is significantly lower than that in the x direction, so our subsequent discussion will focus on the harmonic emission of the x-direction component. Obviously, unlike the harmonic emission in the low energy region, the harmonic spectrum near the cut-off region in the x direction is smoother.

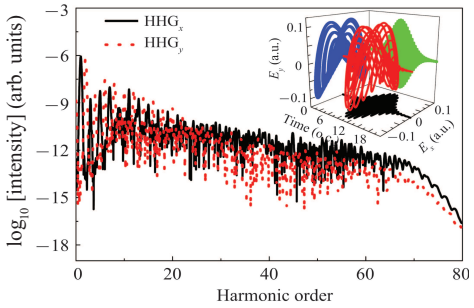


Fig. 1. Harmonic emission spectra of the He atom in an orthogonal two-color linearly polarized field. The black solid line represents the harmonic polarized in the x direction, and the red dashed line is the harmonic polarized in the y direction. The inset shows the form of the electric field.

In Fig. 2 we show that the intensity of the light pulses is changed with time by the superposition of the 65-order–80-order harmonic spectrums in the cut-off region. It can be seen from the Fig. 2(a) that although the driving laser pulse has multiple periods, a strong isolated pulse can still be observed under the condition of this orthogonal two-color field. The FWHM of this pulse is 251 attoseconds, as presented by the black line in the inset of Fig. 2(a). Although there are several pulse transmissions, the intensity of other small pulses is less than half of the intensity of the largest sub-pulse. The interaction between the pulse and the system can still exhibit the characteristics of isolated attosecond interactions. As shown by the red line in the inset of Fig. 2(a), we also calculated the Fourier transform limited duration, which is 155 attoseconds. Because the intensity of the selected high-energy har-

monic is weaker than that of the low-energy harmonic, the synthesized isolated attosecond is wider than the attosecond of the Fourier transform limit. As a comparison, we also calculated the change of the pulse intensity with time, which was synthesized by the same order harmonic spectrum under the action of the monochromatic fundamental frequency linearly polarized pulse, as shown in Fig. 2(b), which is an attosecond pulse train. The FWHM of the pulse with the largest intensity in the attosecond pulse train is 322 attoseconds, as shown in the inset of Fig. 2(b). It can be seen that, compared with the linearly polarized driving laser with the same pulse width, adding a frequency-doubling field in the orthogonal direction can not only effectively suppress the intensity of other subpulses to generate isolated attosecond pulses, but also greatly reduce the pulse width of this attosecond pulse. In order to understand the characteristics of light pulse generation, we carry out wavelet transform on the dipole moments of the system to study the spatiotemporal behavior of its harmonics.

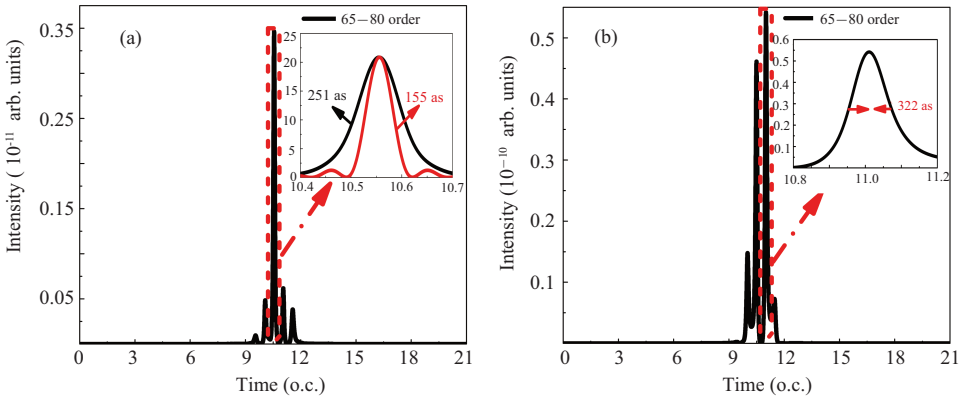


Fig. 2. Attosecond pulse diagram: (a) pulses synthesized from 65th to 80th harmonics under the orthogonal two-color linearly polarized field, (b) pulses synthesized from 65th to 80th harmonics under the monochromatic linearly polarized field.

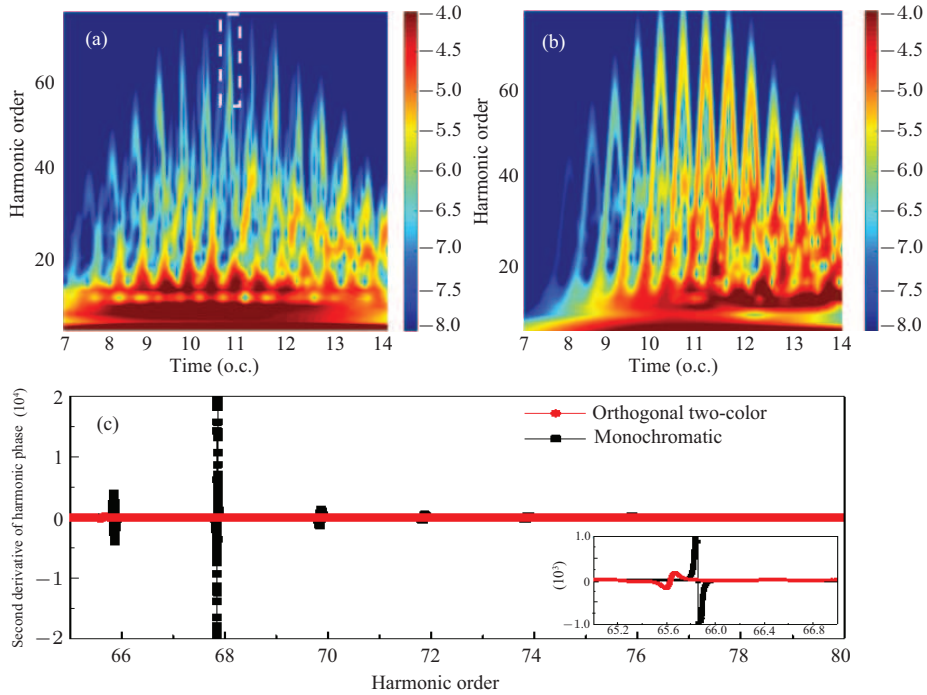


Fig. 3. Time–frequency analysis diagram. (a) The time–frequency analysis diagram of the x direction when the relative phase of the orthogonal two-color linearly polarized field is 0.375 π; (b) The time–frequency analysis diagram of the x direction when the phase of the monochromatic linearly polarized field is 0.375 π. (c) The second derivative diagram of harmonic phase in orthogonal two-color linearly polarized field and monochromatic linearly polarized fields.

Figure 3(a) shows the time–frequency analysis of the orthogonal two-color linearly polarized field with a relative phase of 0.375 π. We also calculated the time–frequency behavior of the harmonics under the action of a monochromatic fundamental frequency linearly polarized pulse, as exhibited in Fig. 3(b). It can be seen from the figure that the maximum energy of the time-dependent harmonic emission by the monochromatic linearly polarized field enhances with the increase of the instantaneous intensity of the driving laser pulse. At the beginning of the pulse, only the long and short trajectories of a single back-nucleation can be observed. With the increase of the time, the contribution of multiple back-

nucleation can be observed in the time–frequency emission spectrum, which makes its harmonic emission behavior more complex. However, in the vicinity of the harmonic cut-off position, it can be observed that the harmonic emission of different half cycles is always contributed by long and short trajectories. In contrast, the harmonic generated by the atom under the action of the orthogonal two-color linearly polarized laser pulse show significantly different behavior. For the platform region, its time–frequency behavior becomes more complex and there are many interference patterns. For the vicinity of the maximum energy, the time-spatial emission behavior is quite different from the linear polarization, and two clear trajectories can no longer be seen, it presents clear characteristics of concentrated harmonic emission, that is, the time of harmonic emission within a certain range is more concentrated, as shown by the time–frequency analysis diagram included in the block in Fig. 3(a). In order to clearly show the harmonic chirp, we calculate the second derivative of the harmonic phase as a function of frequency, as shown in Fig. 3(c). The second derivative of the harmonic phase represents the chirp of the HHG. The smaller the second derivative, the smaller the harmonic chirp.[49] Compared with the monochromatic linearly polarized field (black line), the second derivative of the harmonic phase in the orthogonal two-color fields (red line) is smaller, and it tends to be closer to 0 for the 65-order–80-order harmonics. Therefore, the harmonic chirp of the orthogonal two-color fields is smaller than that of the monochromatic linearly polarized field. We present the second derivative of the harmonic phase with the largest chirp of 65-order–67-order harmonics in the orthogonal two-color fields, as shown in the inset of Fig. 3(c). As can be seen from the figure, a larger chirp appears near the 66th order. From the time–frequency analysis diagram of harmonic emission (Fig. 3(a)), we can see that the harmonic near the 66th order has a low frequency and is located at the intersection of short and long trajectories, and the harmonic emission trajectories of adjacent half periods on both sides also have a small contribution.

In order to understand the time–frequency behavior of this harmonic emission, we further investigate the spatiotemporal evolution of the electronic wave packets, as shown in Fig. 4. In addition to the wave packets evolution, in order to track the motion behavior of ionized electrons more clearly, the spatial distribution of the electron probability flow velocity is further given as $\boldsymbol{j} = -\frac{\mathrm{i}}{2}[\psi^* \hat{p}\psi - \psi \hat{p}\psi^*]$, represented by the arrow in the figure. The length of the arrow indicates the magnitude of the flow rate, and the direction indicates the direction of the movement of the ionized electron. By using classical calculations, we can find a trajectory that produces high-energy harmonics at time 10.58 optical cycles, as shown by the black line in the figure. To explain the motion behavior of the wave packets more clearly, preventing the ionized wave packets at the front and back moments from affecting the motion of the ionized wave packets by the time of 8.28 optical cycles, that is, only the bound state of the wave packets with 8.28 optical cycles is taken, and the ground state is removed when the wave packets evolve to 8.30 optical cycles, and then continues to evolve. The selected time is 8.28–10.60 optical cycles, with an interval of 0.22 optical cycles, and the corresponding time is marked in the figure.

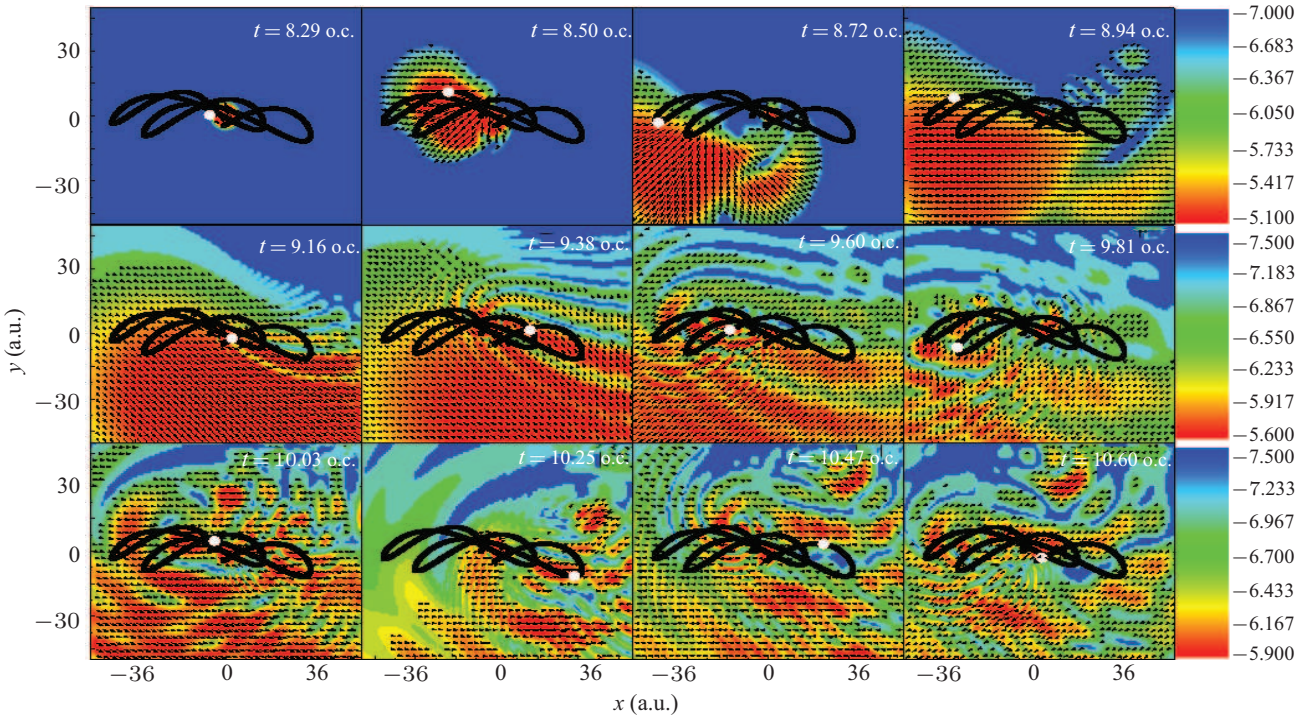


Fig. 4. The wave-packet evolution of the atom in the period of 8.28-optical cycles ionization to 10.58-optical cycles nucleation under the orthogonal two-color linearly polarized fields.

It can be observed from the figure that under the driving of the orthogonal two-color fields, the ionized electron wave packets at this time gradually leave the nuclear region and slowly disperse with time. At the time of the 8.28 optical period, the electron is just beginning to ionize, the direction of the movement of the flow rate is to the upper left and the arrow points outward, indicating that the electrons move away from the nuclear region and move toward the upper left, and the final wave packets return to the nuclear region at the time of 10.60 optical cycles. The motion process of the wave packets under the action of the driving laser pulse is very complex. To facilitate the understanding of the "ionization–motion–recollision" processes of electrons, in Fig. 4, we gave a classic electron motion trajectory returning to the nuclear region corresponding to the above moment. The white circle denotes the position of the ionization electron on the classical trajectory corresponding to the moment. By comparison, it is found that the classical trajectory of the electron is consistent with the behavior of wave-packet motion in this period.

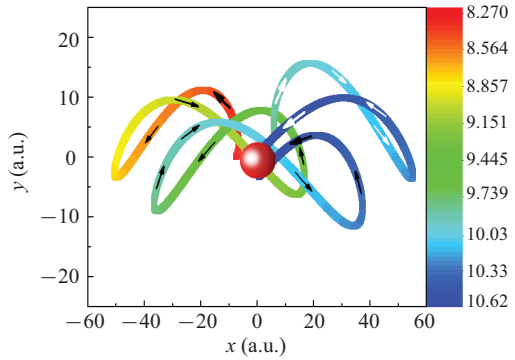


Fig. 5. The classical trajectories of the atom returning to the nucleus at the same time with an optical period of 10.58 in an orthogonal two-color linearly polarized field. The red ball represents the nucleus, and the colors represent the optical cycles.

Using this scheme, we also found that there is another ionization trajectory that can also return to the parent particle to emit harmonics at a time of 10.58 optical cycles, and its ionization initial time is 9.80 optical cycles. Figure 5 shows the position of their classical trajectories as a function of time. The red ball in the middle of the figure represents the nucleus, and the color of the line represents the corresponding time. From the figure, one can notice that a classical trajectory starts from ionization at 8.28 optical cycles and returns to the nucleus at 10.58 optical cycles, corresponding to the ionization of the red part and the return to the nucleus of the blue part. Another classical trajectory is ionization starting from 9.80 optical cycles, 10.58 optical cycles back to the nucleus, corresponding to the turquoise part to the final blue part back to the nucleus. We found that they all return to the nucleus at the same time 10.58 optical cycles. In order to observe this interference process more clearly, we analyzed the behavior of harmonic time–frequency that the dipole moments ionized at different times, as shown in Fig 6. Figure 6(a) presents the time–frequency behavior of the harmonic emission for 10.00–10.80 optical cycles, figure 6(b) displays the time–frequency behavior of the harmonic generated by the wave packets prepared at the time of 8.28 optical cycles, figure 6(c) shows the time–frequency analysis of the harmonic emission generated by the wave packets prepared at the time of 9.80 optical cycles. The luminescence moment of the electron ionized from the time 8.28 optical cycles is in the 10.40–10.70 optical cycles, and the time when the electron ionized from the time 9.80 optical cycles returns to the parent ion to emit high-frequency light is also in this range. Therefore, based on the above analysis, it can be seen that the origin of the quasi-chirp-free emission trajectory is that the two ionized electron wave packets at different times collide with the nucleus at the same time, that is, the interference of the two emission trajectories is generated.

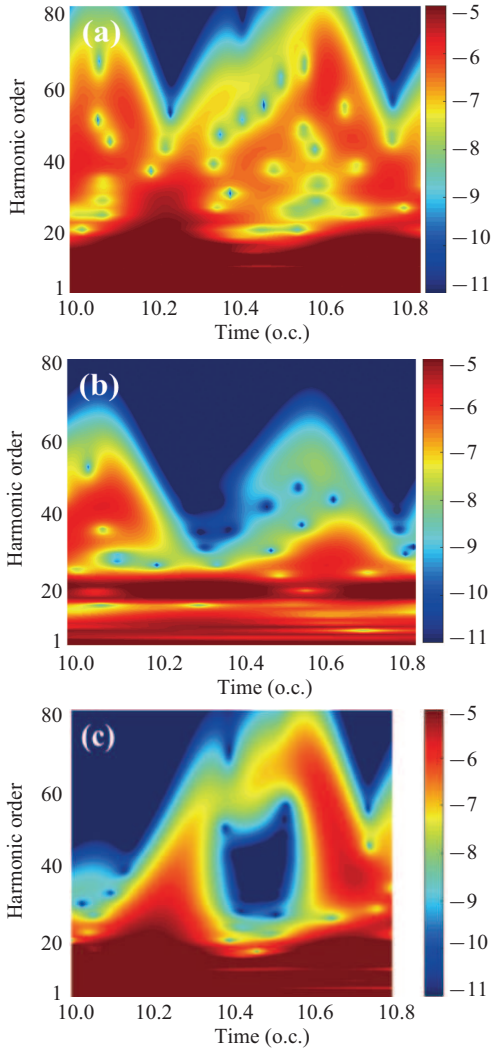


Fig. 6. Time–frequency analysis diagram. (a) Time–frequency analysis of the harmonics from 10.00–10.80 optical cycles. (b) Time–frequency analysis of the harmonics generated by wave packets prepared in 8.28 optical cycles. (c) Time–frequency analysis of the harmonics from wave packets prepared in 9.80 optical cycles.

It can be seen from the above analysis that chirped-free attosecond pulses can be generated when the electrons ionized

at different time scales return to the parent ion at the same time. Since this generation process is closely related to the behavior of electrons driven by the optical field, especially the phase difference between the two driving lasers will play an important role. Next, we focus on analyzing the influence of the relative phase of the two-color linearly polarized fields on the harmonics.

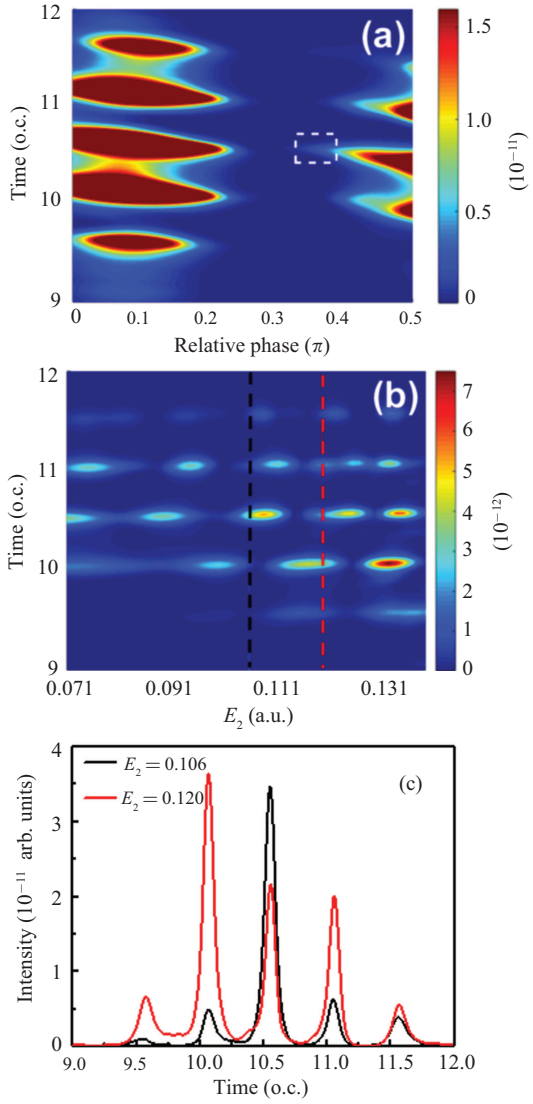


Fig. 7. (a) The change of the attosecond pulse intensity with the relative phase and time. (b) The change of the attosecond pulse intensity with the second laser and time. (c) Attosecond pulse diagrams when $E_2 = 0.106$ (black solid line) and $E_2 = 0.12$ (red solid line).

The relative phase is changed from 0 to 0.5 π. We select the same harmonic energy range, and calculate the variation of the synthesized optical pulse intensity with the phase difference and time, as shown in Fig. 7(a). It can be seen from the diagram, when the phase difference is 0 π, there are pulses are generated in multiple optical cycles. With the increase of the phase, the intensity of the optical pulse gradually decreases. When the phase is 0.35 π–0.38 π, it can be observed that an isolated pulse with a significantly smaller pulse width than the other phases. After further increasing the pulse width, it can be observed that a series of pulses are generated, and the pulse width of the optical pulse becomes larger. It is also observed that when the phase difference is 0.4 π, a pulse with a small pulse width is generated near the time of 11.5 optical cycles, but the intensity of other pulses at this time is large, so it is difficult to observe the generation of isolated ultrashort pulses. This result is consistent with the results of the time–frequency analysis. Different trajectories work under different relative phases, and this method can be used to control the emission trajectory. In addition, we also study the influence of the intensity of the second laser on the attosecond pulse intensity, as shown in Fig. 7(b). By changing the peak amplitude of the double frequency lasers, we find that the number of attosecond pulse neutron pulses can be modulated. For example, when E_2 is 0.106 (black solid line in Fig. 7(c)), the attosecond pulse near $t = 10.58$ o.c. is significantly stronger than other sub-pulses, which can be approximately considered as an isolated single attosecond pulse. In the case of $E_2 = 0.12$ (red solid line in Fig. 7(c)), there are three attosecond pulses with similar intensity at $t = 10.09$ o.c., 10.55 o.c., and 11.07 o.c., and the intensity contrast between sub-pulses of attosecond pulse is also modulated by the double frequency lasers.

4. Conclusions

In conclusion, the harmonic emission of atoms irradiated by the orthogonal two-color linearly polarized pulse is theoretically studied in this paper. It is found that the high-order harmonic near its cut-off energy exhibits small chirp characteristics at a specific phase. By analyzing the wave packet evolution of ionization at different times, electron probability flow, and the classical trajectory of an ionized electron, it is demonstrated that the source of this phenomenon is that the ionized electron wave packets recollide with the nucleus at the same time, the isolated attosecond pulses are synthesized by small chirped harmonic emission in a certain energy range, which lays a theoretical foundation for the generation of shorter attosecond pulses.

Acknowledgments

Project supported by the National Key Research and Development Program of China (Grant No. 2019YFA0307700), the National Natural Science Foundation of China (Grant Nos. 12074145, 11627807, and 11975012), the Research Foundation for Basic Research of Jilin Province, China (Grant No. 20220101003JC), the Fundamental Research Funds for the Central Universities of China (Grant No. 30916011207), and the Outstanding Youth Project of Taizhou University (Grant No. 2019JQ002). We acknowledge the High Performance Computing Center of Jilin University for supercomputer time.

References

[1] Lewenstein M, Balcou P, Ivanov M Y, L'Huillier A and Corkum P B 1994 *Phys. Rev. A* **49** 2117
[2] Protopapas M, Keitel C H and Knight P L 1997 *Rep. Prog. Phys.* **60** 389
[3] Telnov D A, Heslar J and Chu S I 2017 *Phys. Rev. A* **95** 043425
[4] Heslar J, Telnov D A and Chu S I 2017 *Phys. Rev. A* **96** 063404
[5] Qiao Y, Huo Y Q, Liang H Q, Chen J G, Liu W J, Yang Y J and Jiang S C 2023 *Phys. Rev. B* **107** 075201
[6] Yu C, Jiang S C and Lu R F 2019 *Adv. Phys. X* **4** 1562982
[7] Qiao Y, Chen J Q, Huo Y Q, Liang H Q, Yu R X, Chen J G, Liu W J, Jiang S C and Yang Y J 2023 *Phys. Rev. A* **107** 023523
[8] Wu T, Qian C, Wang Z S, Zhang X Y, Yu C and Lu R F 2022 *Acta Photon. Sin.* **51** 0851515
[9] McPherson A, Gibson G, Jara H, Johann U, Luk T S, McIntyre I A, Boyer K and Rhodes C K 1987 *J. Opt. Soc. Am. B* **4** 595
[10] Qiao Y, Wu D, Chen J G, Wang J, Guo F M and Yang Y J 2019 *Phys. Rev. A* **100** 063428
[11] Qiao Y, Huo Y Q, Jiang S C, Yang Y J and Chen J G 2022 *Opt. Express* **30** 9971
[12] Odžak S, Hasović E and Milošević D B 2016 *Phys. Rev. A* **94** 033419
[13] Li P, Gao N, Yu R X, Wang J, Li S Y, Guo F M and Yang Y J 2022 *Chin. Phys. B* **31** 103303
[14] Qiao Y, Chen J Q and Chen J G 2022 *Symmetry* **14** 2646
[15] Zhou S S, Lan W D, Chen J G, Wang J, Guo F M and Yang Y J 2022 *Phys. Rev. A* **106** 023510
[16] Yan J Z, Zhao S S, Lan W D, Li S Y, Zhou S S, Chen J G, Zhang J Y and Yang Y J 2022 *Opt. Express* **30** 35444
[17] Haight R and Seidler P F 1994 *Appl. Phys. Lett.* **65** 517
[18] Sandhu A S, Gagnon E, Santra R, Sharma V, Li W, Ho P, Ranitovic P, Cocke C L, Murnane M M and Kapteyn H C 2008 *Science* **322** 1081
[19] Siemens M E, Li Q, Yang R, Nelson K A, Anderson E H, Murnane M M and Kapteyn H C 2010 *Nat. Mater.* **9** 26
[20] La-O-Vorakiat C, Siemens M, Murnane M M, Kapteyn H C, Mathias S, Aeschlimann M, Grychtol P, Adam R, Schneider C M, Shaw J M, Nembach H and Silva T J 2009 *Phys. Rev. Lett.* **103** 257402
[21] Sandberg R L, Raymondson D A, o vorakiat C L, Paul A, Raines K S, Miao J, Murnane M M, Kapteyn H C and Schlotter W F 2009 *Opt. Lett.* **34** 1618
[22] Hentschel M, Kienberger R, Spielmann C, Reider G A, Milosevic N, Brabec T, Corkum P, Heinzmann U, Drescher M and Krausz F 2001 *Nature* **414** 509
[23] Li J, Ren X M, Yin Y C, Zhao K, Chew A, Cheng Y, Cunningham E, Wang Y, Hu S Y, Wu Y, Chini M and Chang Z H 2017 *Nat. Commun.* **8** 186
[24] Paul P M, Toma E S, Breger P, Mullot G, Augé F, Balcou P, Muller H G and Agostini P 2001 *Science* **292** 1689
[25] Mairesse Y, De Bohan A, Frasinski L, Merdji H, Dinu L, Monchicourt P, Breger P, Kovacev M, Taïeb R, Carré B, Mulle H, Agostini P and Saliéres P 2003 *Science* **302** 1540
[26] Corkum P B 1993 *Phys. Rev. Lett.* **71** 1994
[27] Schafer K J, Yang B, DiMauro L F and Kulander K C 1993 *Phys. Rev. Lett.* **70** 1599
[28] Sekikawa T, Ohno T, Yamazaki T, Nabekawa Y and Watanabe S 1999 *Phys. Rev. Lett.* **83** 2564
[29] Popmintchev T, Chen M C, Popmintchev D, *et al.* 2012 *Science* **336** 1287
[30] Gaumnitz T, Jain A, Pertot Y, Huppert M, Jordan I, Ardana-Lamas F and Wörner H J 2017 *Opt. Express* **25** 27506
[31] Morlens A S, Balcou P, Zeitoun P, Valentin C, Laude V and Kazamias S 2005 *Opt. Lett.* **30** 1554
[32] Kim K T, Kim C M, Baik M G, Umesh G and Nam C H 2004 *Phys. Rev. A* **69** 051805
[33] Lopez-Martens R, Varjú K, Johnsson P, Mauritsson J, Mairesse Y, Salieres P, Gaarde M B, Schafer K J, Persson A, Svanberg S, Claes-G?ran W and L'Huillier A 2005 *Phys. Rev. Lett.* **94** 033001
[34] Ko D H, Kim K T, Park J, Lee J h and Nam C H 2010 *New J. Phys.* **12** 063008
[35] Kim K T, Kang K S, Park M N, Imran T, Umesh G and Nam C H 2007 *Phys. Rev. Lett.* **99** 223904
[36] Zou P, Zeng Z N, Zheng Y H, Lu Y Y, Liu P, Li R X and Xu Z Z 2010 *Phys. Rev. A* **81** 033428
[37] Kohler M C, Keitel C H and Hatsagortsyan K Z 2011 *Opt. Express* **19** 4411
[38] Wang J, Chen G, Li S Y, Ding D J, Chen J G, Guo F M and Yang Y J 2015 *Phys. Rev. A* **92** 033848
[39] Jia C, Wang J, Li Q Y, Guo F M, Chen J G, Zeng S L and Yang Y J 2015 *Opt. Express* **23** 32222
[40] Balogh E, Kovacs K, Dombi P, Fulop J A, Farkas G, Hebling J, Tosa V and Varju K 2011 *Phys. Rev. A* **84** 023806
[41] Yuan K J and Bandrauk A D 2013 *Phys. Rev. Lett.* **110** 023003
[42] Ge X L, Du H, Guo J and Liu X S 2015 *Opt. Lett.* **23** 8837
[43] Kim I J, Kim C M, Kim H T, Lee G H, Lee Y S, Park J Y, Cho D J and Nam C H 2005 *Phys. Rev. Lett.* **94** 243901
[44] Kim C M, Kim I J and Nam C H 2005 *Phys. Rev. A* **72** 033817
[45] Zheng Y H, Zeng Z N, Zou P, Zhang L, Li X F, Liu P, Li R X and Xu Z Z 2009 *Phys. Rev. Lett.* **103** 043904
[46] Wang J, Chen G, Guo F M, Li S Y, Chen J G and Yang Y J 2013 *Chin. Phys. B* **22** 033203
[47] Yang Y J, Chen J G, Huang Y X, Guo F M, Zhang H X, Sun J Z, Zhu H Y, Li W, Wang H and Zhu Q R 2007 *Chin. Phys. Lett.* **24** 1894
[48] Guo F M, Yang Y J, Jin M X, Ding D J and Zhu Q R 2009 *Chin. Phys. Lett.* **26** 053201
[49] Kazamias S and Balcou P 2004 *Phys. Rev. A* **69** 063416